Percolation Description of the Global Topography of Earth and the Moon

Abbas Ali Saberi[*]

Department of Physics, College of Science, University of Tehran, P.O. Box 14395-547, Tehran, Iran
Institut für Theoretische Physik, Universität zu Köln, Zülpicher Straße 77, 50937 Köln, Germany
(Received 13 August 2012; published 24 April 2013)

Remarkable global correlations exist between geometrical features of terrestrial surfaces on Earth, current mean sea level, and its geological internal processes whose origins have remained an essential goal in the earth sciences. Theoretical modeling of the ubiquitous self-similar fractal patterns observed on Earth and their underlying rules is indeed of great importance. Here I present a percolation description of the global topography of Earth in which the present mean sea level is automatically singled out as a critical level in the model. This finding elucidates the origins of the appearance of scale invariant patterns on Earth. The criticality is shown to be accompanied by a continental aggregation, unraveling an important correlation between the water and long-range topographic evolutions. To have a comparison point in hand, I apply such an analysis to the lunar topography which reveals various characteristic features of the Moon.

Discovering the connection between geometrical features of terrestrial surfaces on Earth and its geological internal processes has long been a basic challenge area in the earth sciences [1,2], and has attracted the attention of physicists and mathematicians as well [3]. Various theoretical models have emerged to identify the underlying constructive rules responsible for the appearance of self-similarity, scale, and conformal invariance in the fractal geometry of local geomorphic patterns [4–9]. In comparison with different models proposed to describe the statistical properties of regional features [10–12], the global topography has received less attention and thus remained controversial. Here I show that the global surface topography can be well described by percolation theory, the simplest and a fundamental model in statistical mechanics that exhibits phase transitions. A dynamic geoidlike level is defined as an equipotential spherical surface as a counterpart of the percolation parameter. The analysis shows a geometrical phase transition in which the critical level surface directly corresponds to the present mean sea level on Earth, automatically singling this level out. This may shed new light on the tectonic plate motion and help unravel the dynamic story of Earth's interior. As a comparison, I also present its application to the lunar topography.

Scale invariance is a remarkable feature of Earth's surface topography. Observations [13–16] indicate that, over a wide range of scales, the power spectrum S of linear transects of Earth's topography follows the scaling relation $S \propto k^{-2}$ with the wave number k. Such a power law spectrum in the topography leads to the corresponding iso-height lines (such as coastlines) being fractal sets characterized by a dominant fractal dimension of $4/3$ [3,4,17]. Many other ubiquitous scaling relations observed in the various terrestrial features, e.g., in the radiation fields of volcanoes [18,19], surface magnetic susceptibility [20],

geomagnetism [21], and surface hydrology such as in the river basin geomorphology [22], are all relevant to the wide range scale invariance of the topography. Nevertheless, further surveys based on the fractional Brownian motion model [14] of topography or bathymetry [23] revealed a more complex multifractal structure of Earth's morphology giving rise to distinct scaling properties of oceans, continents, and continental margins [7]. Such a difference is also evident in the well-known bimodal distribution of Earth's topography [24] that reflects the topographic dichotomy of continents and ocean basins, a consequence of plate tectonic processes.

Plate tectonic theory provides a framework that explains most of the major surface topographic features of Earth. It also accounts for the connection between the processes that facilitate heat loss and the forces that drive plate motion. The distribution of the plate areas covering Earth has been shown to be a power law with exponent ~ 0.25 for all plates [25,26]. A remarkable relationship that provides one of the cornerstones of plate tectonics is that, to a very good approximation, the depth of the ocean floor beneath the ridge crest increases with the square root of the age of the ocean floor, at least for an ocean lithosphere younger than about 80 Myr [27]. It plays an important role in topographical changes and fundamentally affects long-term variations in global sea level that would assume a surface equal to the geoid. Here I present the results of a statistical analysis based on percolation theory that provides new insight into the better understanding of various interrelationships between the above mentioned issues and their origins.

I use the topographic data available for the global relief model of Earth's surface that integrates land topography and ocean bathymetry [28] (the data information is presented in Ref. [29]). The current mean sea level is assumed as a vertical datum of the height relief which means that the data consider the imperfect ellipsoidal shape of Earth.

The height relief $\mathfrak{h}(r, \theta, \phi)$ is therefore assumed on a sphere of unit radius $r = 1$, that also coincides with the present mean sea level (as zero height level) on Earth. All corresponding lengths here are expressed in units of Earth's average radius.

Now imagine flooding this global landscape in a way that the continental land masses were crisscrossed by a series of narrow channels so that the resulting sea level all over Earth would coincide with a spherical surface—the geoid. All parts above the water level are then colored differently as disjoint islands, and the rest is left white (Fig. 1). If the water level is high, there will be small disconnected islands, and if it is low, there will be disconnected lakes. However, there may be a critical value of the sea level $\mathfrak{h} = h_c$ at which a percolation transition takes place [30,31].

The percolation problem [31,32] is an example of the simplest pure geometrical phase transitions with nontrivial critical behavior, and it is closely related to the surface topography [33,34]. At the critical point in two dimensions, the percolation clusters are some fractal objects whose outer perimeter is described by a fractal dimension of 4/3. By considering the dynamic sea level (height) as a

percolation parameter, I examine a possible description of Earth's topography by means of the percolation theory.

The first quantity of interest is the total length of the coastlines at varying altitude (or sea level) which is shown in Fig. 2. In all figures, the error bars are of the same order as the symbol size [35]. Having looked at Fig. 2, this quantity closely resembles the height distribution function of Earth and the Moon [36]. The one for Earth is characterized by the presence of two levels centered around the elevations 320 and -4280 m in the continental platforms and oceanic floors, respectively. The ratio of the total length of the coastlines at 320 m to the zero height level is $\sim$2.71. Unlike Earth, the Moon's curve features only a single peak at around -1080 m.

The usual order parameter is defined as the probability of any site to be part of the largest island. As shown in Fig. 3, the order parameter for islands has a sharp dropoff around the zero height level, i.e., right at the present mean sea level. According to the further evidence given in the following, it is an indicative of a geometrical phase transition at this level. The same analysis for the oceanic clusters (where disjoint oceans at each level are differently colored, leaving islands white) gives rise to a discontinuous jump in the oceanic order parameter at around -3640 m (Fig. 3).

Figure 4 illustrates two other percolation observables measured for Earth, the mean island size (analogous to the susceptibility of the system), and the correlation length. The mean island size χ is defined as $\chi = \sum_{s}' s^2 n_s(h)/\sum_{s}' s n_s(h)$, where $n_s(h)$ denotes the average number of islands of size s at level h, and the prime on the sums indicates the exclusion of the largest island in each measurement. The correlation length ξ is also defined as the average distance of sites belonging to the same island, $\xi^2 = \sum_{s}' 2 R_s^2 s^2 n_s(h)/\sum_{s}' s^2 n_s(h)$, where R_s is the

FIG. 1 (color online). Schematic illustration of the continental aggregation by decreasing the sea level from top to bottom. The first four snapshots are selected around the remarkable percolation transition at the present mean sea level around which the major parts of the landmass join together. This is followed by three other levels indicating the junction of Greenland, Australia, and Antarctica to the giant landmass. The lowest right figure shows the longitudinal percolation of the oceanic clusters (see the Supplemental Material [37] for enlarged figures and also for the ones at additional sea levels).

FIG. 2 (color online). The total length of the coastlines as a function of the sea level (or height) for Earth (main panel) and the Moon (inset).
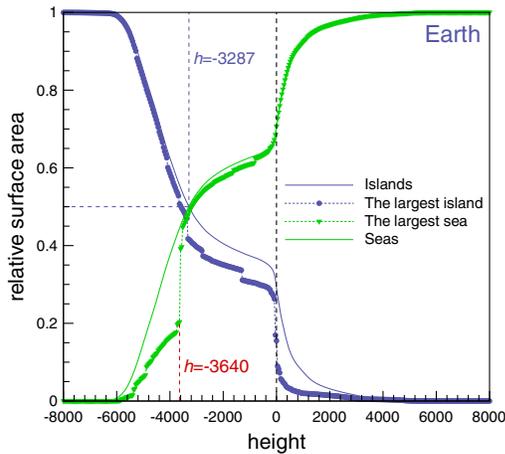
FIG. 3 (color online). Relative surface area of the largest
island (circles) and the largest sea (triangles) followed by the
total surface area of the islands and the oceans (solid lines) to the
total area 4π of Earth, as a function of the sea level. One critical
level is distinguished by each order parameter. The oceanic
critical level is close to the level $h = -3287$ m at which the
total island and oceanic surface areas are equal.

radius of gyration of a given s cluster. As shown in Fig. 4,
both quantities χ and ξ become divergent at the present
mean sea level. The divergence of the correlation length is
a signature of a continuous phase transition at this level,
implying that the critical fluctuations dominate at each
length scale and that the system becomes scale invariant.
These results provide a strong correlation between the
water and long-range topographic evolutions on Earth.
Nevertheless, one may imagine a model in which water
itself—through erosion, evaporation, precipitation, and

sedimentation, etc.—may have an active role in shaping
topography, i.e., the activity of water itself with resulting
plains of little height, shapes the landscape to appear
critical around the zero height.

The measurement of χ and ξ for the oceanic clusters
shows a dominant divergence that signals the oceanic
critical level already observed in Fig. 3. The mean ocean
size reaches its absolute maximum at this critical level and
the correlation length remains approximately constant at
its maximum for level interval $-4280 \lesssim h \lesssim -3760$ (see
the Supplemental Material [37]).

Figure 1 is an illustration of the percolation transition
at the present mean sea level. As can be seen from the
figure, all major continental junctions occur at the level
interval $-80 \lesssim h \lesssim +80$. At a sea level around -760 m,
Greenland joins the Afro-Eurasia supercontinent to the
Americas and at the same level the total length of the
coastlines reaches its minimum (Fig. 2). The continents
Australia and Antarctica join to the landmass at -1320 and
-3360 m, respectively (Fig. 1).

In order to have a reference point for comparison, as an
example of the most heavily studied waterless body with a
completely different surface properties and interior mecha-
nism, let me analyze the lunar topography. I used the
topogrd2 data set (accessible from Ref. [38]), which is
measured relative to a spheroid of radius 1738 km at the
equator—the zero height level. I rescale the Moon's aver-
age radius to 1.

The percolation observables discussed above for the
islands are measured as a function of a hypothetical sea

FIG. 4 (color online). Correlation length and mean island
(land) size vs the sea level, with a remarkable characterization
of a geometrical phase transition at the present mean sea level
(zero hight level). The scale factors by which all the numbers
labeling the vertical axis should be multiplied to get the correct
graph units are the radius and the square of the radius of Earth
for ξ and χ, respectively.

FIG. 5 (color online). Relative surface area of the largest island
followed by the total surface area of the islands to the total area 4π
of the Moon, as a function of the hypothetical sea level. At level
~ -1049 m, the total island and oceanic surface areas on the
Moon are equal. The two jumps in the order parameter at levels
around -960 and 1360 m are also decoded in the divergent
behavior of the correlation length and the mean island size (the
inset). Such two jumps are unusual for percolation.
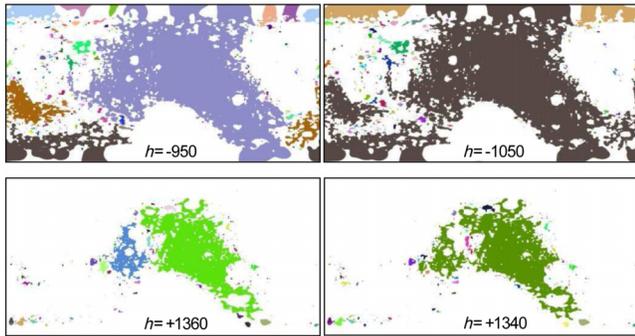
FIG. 6 (color online). Upper: Disjoint islands with heights higher than the hypothetical sea level on the Moon for two different levels $h = -950$ and -1050 m, slightly above and below the critical level, respectively. Appearance of the spanning island (right figure) is indicative of a percolation transition. Lower: Aggregation of the two main mountainous islands at the lunar farside around the second critical level at ~ 1360 m.

level (Fig. 5). The order parameter shows two rather small jumps at altitude levels around -960 and 1360 m. The correlation length and the mean island size have also two dominant peaks at these levels (see the inset of Fig. 5). The Moon's height distribution function features a single global peak at level ~ -950 m which is quite close to the one of the critical levels located at ~ -960 m. In addition, if we measure the correlation length and the mean cluster size for the oceanic clusters, they show only one critical level very close to the one located at ~ -960 m. These may imply that this critical level is more important for the description of the global topography of the Moon. This is also quite close to the level $h = -1049$ m at which the total island and oceanic surface areas are equal, meaning that the island and oceanic percolation thresholds coincide.

The illustrative Fig. 6 shows the connectivity of the islands on both sides of the critical level. At a height level $h = -950$ m, a little above the critical level, there exists a number of disjoint islands. At slightly below the critical level at $h = -1050$ m, the islands merge together to form a giant percolating island which spans the Moon in the longitudinal direction.

Nevertheless, the other critical level at $h = 1360$ m, unravels a characteristic feature of the lunar farside. As it is known, one of the most striking geological features of the Moon is the elevation dichotomy [39] between the hemispheres: the nearside is low and flat, dominated by volcanic maria, whereas the farside is mountainous and deeply cratered. The illustrations in Fig. 6 for elevation levels at $h = 1360$ and 1340 m, at both sides of the critical level, indicate the aggregation of two main mountainous islands that are separated by a very narrow passageway. This may be a benchmark of a rather nonrandom origin of the formation of the lunar farside highlands [40].

To summarize, the percolation description of Earth's global topography uncovers the important role that is played by water on Earth. The critical threshold of the model coincides with the current mean sea level on Earth. This criticality is along with a sign of the continental aggregation at this level which seems to be more dominated by the *endogenic* processes (like volcanic activity, earthquakes, and tectonic processes) originating within Earth that are mainly responsible for the very long-wavelength topography of Earth's surface, rather than by the *exogenic* processes like erosion, weathering, and precipitation. The criticality of the current sea level also justifies the appearance of the scale (and conformal) invariant features on Earth with an intriguing coincidence of the dominant 4/3 fractal dimension in the critical model and observation. The main critical level for the Moon has the same amount of land and oceans at the threshold, indicating a purely geometrical phase transition.

*ab.saberi@ut.ac.ir

[1] C. Lyell, *The Principles of Geology; or, The Modern Changes of the Earth and its Inhabitants Considered as Illustrative of Geology* (Murray, London, 1830), Vol. 3.

[2] A. Cazenave, A. Souriau, and K. Dominh, Nature (London) **340**, 54 (1989).

[3] J. Perrin, *Les atomes* (NRF-Gallimard, Paris, 1913).

[4] B. B. Mandelbrot, Science **156**, 636 (1967).

[5] B. B. Mandelbrot, *The Fractal Geometry of Nature* (W. H. Freeman, New York, 1983).

[6] J.-S. Gagnon, S. Lovejoy, and D. Schertzer, Europhys. Lett. **62**, 801 (2003).

[7] J.-S. Gagnon, S. Lovejoy, and D. Schertzer, Nonlinear Proc. Geophys. **13**, 541 (2006).

[8] A. Baldassarri, M. Montuori, O. Prieto-Ballesteros, and S. C. Manrubia, J. Geophys. Res. **113**, E09002 (2008).

[9] G. Boffetta, A. Celani, D. Dezzani, and A. Seminara, Geophys. Res. Lett. **35**, L03615 (2008).

[10] C. P. Stark, Nature (London) **352**, 423 (1991).

[11] A. Maritan, F. Colaiori, A. Flammini, M. Cieplak, and J. R. Banavar, Science **272**, 984 (1996).

[12] B. Sapoval, A. Baldassarri, and A. Gabrielli, Phys. Rev. Lett. **93**, 098501 (2004).

[13] F. A. Vening Meinesz, Proc. Koninkl. Ned. Akad. Wetensch., Ser. B **55**, 212 (1951).

[14] B. Mandelbrot, Proc. Natl. Acad. Sci. U.S.A. **72**, 3825 (1975).

[15] R. S. Sayles and T. R. Thomas, Nature (London) **271,** 431 (1978).

[16] J. D. Pelletier, J. Geophys. Res. **104,** 7359 (1999).

[17] H. Steinhaus, Colloquium Mathematicum **3,** 1 (1954).

[18] D. C. Harvey, H. Gaonach, S. Lovejoy, J. Stix, and D. Schertzer, Fractals **10,** 265 (2002).

[19] H. Gaonach, S. Lovejoy, and D. Schertzer, Int. J. Rem. Sens. **24,** 2323 (2003).

[20] M. Pilkington and J. Todoeschuck, Geophys. Res. Lett. **22,** 779 (1995).

[21] S. Pecknold, S. Lovejoy, and D. Schertzer, Geophys. J. Int. **145,** 127 (2001).

[22] I. Rodriguez-Iturbe and A. Rinaldo, *Fractal River Basins: Chance and Self-Organization* (Cambridge University Press, Cambridge, England, 1997).

[23] Bathymetry is the underwater equivalent to topography.

[24] A. Wegener, in *The Origin of Continents and Oceans*, edited by J. Biram (Dover, New York, 1966), translated from the 1929 4th German ed.

[25] P. Bird, Geochem., Geophys., Geosyst. **4,** 1027 (2003).

[26] D. Sornette and V. F. Pisarenko, Geophys. Res. Lett. **30,** 1105 (2003).

[27] D. L. Turcotte and G. Schubert, *Geodynamics, Application of Continuum Physics to Geological Problems* (John Wiley & Sons, New York, 1982).

[28] C. Amante and B. W. Eakins, NOAA Technical Memorandum NESDIS NGDC-24, 2009.

[29] http://www.ngdc.noaa.gov/mgg/global/global.html.

[30] J. Cardy, Nat. Phys. **2,** 67 (2006).

[31] M. Sahimi, *Applications of Percolation Theory* (Taylor & Francis, London, 1994).

[32] D. Stauffer and A. Aharony, *Introduction to Percolation Theory* (Taylor & Francis, London, 1994), 2nd ed.

[33] A. A. Saberi, M. A. Rajabpour, and S. Rouhani, Phys. Rev. Lett. **100,** 044504 (2008).

[34] A. A. Saberi, Appl. Phys. Lett. **97,** 154102 (2010).

[35] The ETOPO1 global relief model has an accuracy of about 10 meters at best, likely less accurate in the deep ocean. Part of the reason for the large error bars is that each cell's elevation value represents the average elevation over the entire roughly 2×2 km^2 footprint of the cell [28]. All mentioned height levels here would indeed bear such uncertainties.

[36] P. R. Stoddard and D. M. Jurdy, Icarus **217,** 524 (2012).

[37] See Supplemental Material at http://link.aps.org/supplemental/10.1103/PhysRevLett.110.178501 for enlarged schematic illustrations of land and oceanic clusters at various sea levels, and the same computations of Fig. 4 for oceanic clusters on Earth.

[38] http://pds-geosciences.wustl.edu/missions/clementine/gravtopo.html.

[39] M. T. Zuber, D. E. Smith, F. G. Lemoine, and G. A. Neumann, Science **266,** 1839 (1994).

[40] M. Jutzi and E. Asphaug, Nature (London) **476,** 69 (2011).